

Instituto Tecnológico y de Estudios Superiores de Monterrey
Campus Guadalajara
School of Engineering and Sciences

Independent Study
Elbow Control Synergies

Submitted by:
Roderico Alfredo García Leal

Main advisor:
Dr. Joel Huegel

Internship Program:
ETH Robotics Summer Fellowship

Hosting Laboratory:
Sensory Motor Systems Lab

Supervisor:
Dr. Robert Reiner

Tutors:
Yves Zimmerman
Michael Sommerhalder

Guadalajara, December 3rd 2022

Abstract

Nowadays, robotics has achieved a high degree of development. This technology has found to be useful in more challenging applications, such is the case of rehabilitation. These devices replicate the kinematic chain of the human arm, presenting a kinematic redundancy due to the high number of DOF. The use of the swivel angle has been a common approach in the literature for the solution of this kinematic redundancy. A cost function is proposed to estimate a human-like elevation angle of the elbow at a given position and orientation of the hand. This function is intended to be used in the ANYexo, a novel upper-limb exoskeleton. Since the ANYexo fulfills all the DOF of the human arm, it is desired to solve the elbow redundancy. To achieve this, a dataset with kinematic data of humans performing activities of daily life using their arm was analyzed. The arm of each subject was reconstructed with the purpose of calculating the elevation of the elbow in every posture they took during each one of the tasks. The proposed cost function was developed in such a way that it considers both the desired orientation and cartesian position for the hand, or end effector in the case of an exoskeleton. Depending on the given weight to each of these parameters, an optimal elbow elevation angle was computed and extracted from the pre-processed data of the subjects. The obtained results are the first steps for the generation of human-like trajectories in exoskeletons such as the ANYexo.

Contents

1	Introduction	5
1.1	Theoretical background	5
1.2	The ANYexo	7
1.3	The U-LIMB database	7
1.4	Contribution	8
2	Methodology	9
2.1	Analysis Pipeline	9
2.2	Kinematic Data	9
2.2.1	Data filtering	11
2.2.2	Redefinition of the world coordinates	11
2.3	Arm reconstruction	11
2.4	Elbow elevation angle	14
2.5	Axis Rotation Angle	14
2.6	Swivel angle database	16
2.6.1	Clustering data by arm length	16
2.7	Cost function for estimation of swivel angle	17
2.8	Standard deviation based in a maximum distance	18
3	Results	19
3.1	Evaluating distance function	19
3.2	Gaussian distribution of distance data	21
3.3	Swivel angle along a trajectory	22
4	Discussion	25
4.1	Interpretation of results	25
4.2	Limitations and improvements	26
5	Conclusion	26

List of Figures

1	Pipeline for the estimation of optimal elbow elevation angle (swivel angle).	9
2	Anatomical placement of active markers, and details on the marker support used for the experiments at UP. Numerical values on the dimensions of marker support are reported in millimeters [1]	11
3	Definition of the swivel angle [2]	12
4	Visualization of the vector v_a , $v_f a$ and v_h obtained from the marker's data.	13
5	Example of a subject's arm reconstructions. World reference frame (WRF) place at the shoulder, and hand's reference frame (HRF) placed at the center of the hand.	14
6	Vector v_{nz} and v_{sw} form the plane p_1 , and vector v_{sw} and v_{se} form the plane p_2 . Angle between planes p_1 and p_2 form the swivel angle.	15
7	Arm length histogram of the 39 participants from the UP database.	17
8	a) Scatter plot showing the distance function evaluated at the desired hand pose. ADLs identified by color and maker type. b) Scatter plot only displaying values below the maximum tolerated distance d_{max}	20
9	a) Gaussian distribution in combination with a straight line starting at the inflection point of the curve. b) Data points below the d_{max} threshold.	22
10	Swivel angle progression for a movement mimicking the action of taking food to the mouth. a) $d_{max} = 0.15$. b) $d_{max} = 0.2$. c) $d_{max} = 0.25$	23
11	Swivel angle progression for a movement mimicking the action of moving the hand from left to right side at the shoulder level. a) $d_{max} = 0.15$. b) $d_{max} = 0.2$. c) $d_{max} = 0.25$	23
12	Swivel angle progression for a movement mimicking the action of placing the hand on the right side, fingers pointing upwards and arm forming an 'L' shape, turning the arm until the palm face downwards. a) $d_{max} = 0.15$. b) $d_{max} = 0.2$. c) $d_{max} = 0.25$	23
13	Swivel angle progression for a movement mimicking the action of displacing the hand from right to left along a surface below the shoulder level. a) $d_{max} = 0.15$. b) $d_{max} = 0.2$. c) $d_{max} = 0.25$	23
14	Swivel angle progression for a movement mimicking the action of pouring water into a container placed on a table in front of the subject. a) $d_{max} = 0.15$. b) $d_{max} = 0.2$. c) $d_{max} = 0.25$	24
15	Swivel angle progression for a movement mimicking the action of a 'thumb up' expression, placing the hand in front of the subject. a) $d_{max} = 0.15$. b) $d_{max} = 0.2$. c) $d_{max} = 0.25$	24

16	Swivel angle progression for a movement mimicking the action of a 'thumb down' expression, placing the hand in front of the subject. a) $d_{max} = 0.15$. b) $d_{max} = 0.2$. c) $d_{max} = 0.25$.	24
17	Swivel angle progression for a movement mimicking the action of reaching the top of the head with the palm. a) $d_{max} = 0.15$. b) $d_{max} = 0.2$. c) $d_{max} = 0.25$.	24
18	Swivel angle progression for a movement mimicking the action of reaching the left shoulder with the finger tips. a) $d_{max} = 0.15$. b) $d_{max} = 0.2$. c) $d_{max} = 0.25$.	24
19	Swivel angle progression for a movement mimicking the action of waving the hand at the same position, only moving the wrist joint. a) $d_{max} = 0.15$. b) $d_{max} = 0.2$. c) $d_{max} = 0.25$.	25

List of Tables

1	List of activities or daily living (ADL) performed by the subjects [1]	10
2	Format of stored processed data for each subject.	16

1 Introduction

1.1 Theoretical background

In the last decades, robots have achieved a high grade of development, being able to perform tasks with a high level of precision. Thanks to their improvement through the years, robots have started to be used in more challenging applications, such as collaborative robots, as well as in human rehabilitation.

When robots are used for these applications, either collaborative tasks, rehabilitation, or human augmentation, an adequate Human-Robot Interaction (HRI) is required. A proper human-machine interaction allows the user to feel confidence when interacting with the system. The safety of a robot involves not only the control and sensing of the movements, but also the motion profiles executed by the robot when performing a task. The HRI is highly improved when robot manipulators resemble human-like behaviour at the kinematics level [2], since this makes easier to the user to predict the movements of the device.

In the field of rehabilitation engineering, exoskeletons are commonly used to assist users to perform rehabilitation therapies. Exoskeletons are wearable devices that are attached to the user proving a 3D interaction. The kinematic design of exoskeletons pretend to replicate the human limb kinematics, by aligning the mechanism joints to those in the human body [3]. However, by doing so, kinematic redundancy, as in the human limbs, present in the robotic device.

Kinematics redundancy appears when an articulate robot has more than six degrees of freedom (DOF). This presents a problematic since there is not unique inverse kinematic solution for these type of manipulators. In upper limb exoskeletons, for example, the literature shows that a robot with a 7-DOF configuration is commonly used to replicate the human arm kinematics. The first 3-DOF are for the shoulder spherical joint, 1-DOF for the elbow, and finally 3-DOF for the wrist spherical joint. This kinematic configuration, as explained before, gives place to a kinematic redundancy.

Upper limb exoskeletons are commonly used for rehabilitation purposes. For these type of application, it is crucial to achieve a HRI that allows the user to perform human-like movements in order to have a proper recovery of his/her motor capabilities. To achieve movement profiles similar to the human ones, kinematics redundancy needs to be solved.

The redundancy of the human arm has remarkable advantages for everyday activities. For example, the kinematic chain of the arm has enough DOFs for us to keep performing essential functions even if one or more joints are constrained or dysfunctional [4]. However, the way human motor control resolves the arm redundancy has not been fully understood. Several studies have been made to study the human motion, starting from simple kinematics analysis, to complex neuromuscular studies. It has been found that the nervous systems uses neural strategies to simplify the dimensionality of the motor control. This is known as

synergies, which was defined by Latash et. al [5] as a neural organization resulting in task specific co-variation of elements variables, with the ultimate goal of generating stable and effective movements. As a result, the amount of components to control when performing a movement is less than the number of elements resulting from a mechanical count [6].

Cost functions have been proposed to describe human-like movements. One of the approaches was the use of jerk minimization to obtain natural trajectories for the human arm [7]. In [8], the kinematic redundancy of the arm was resolved by minimizing the magnitude of the total work done by each one of the joint torques. Finally, the use of the swivel angle has also been a common approach to solve the arm kinematic redundancy when performing reaching tasks.

The swivel angle is defined as the angular rotation of the elbow around an axis that passes through the shoulder and wrist joints. When locking the hand in a specific position and orientation, the arm is able to rotate around two constrained points: the shoulder and the wrist, being possible to place the elbow at different elevation angles. By calculating the optimal swivel angle, the kinematic redundancy of the arm can be resolved. This elbow elevation when performing tasks has been studied for several years. In 2002, Kang et al. [9] measured the swivel angle of two right-handed healthy subjects when reaching objects at different horizontal and vertical positions. With this study, it was concluded that the elbow swivel angle significantly and systematically depends on the target coordinates.

In [4], it was hypothesized that the swivel angle is selected by the motor control system to efficiently retract the palm to the head region. Considering this hypothesis, the optimal swivel angle was computed in function to maximize the projection of the palm towards the head. The estimation of the swivel angle was compared with kinematic data of healthy subjects performing reaching tasks. A cost function, explained in the following section, was used to compute the elbow elevation taking as reference the wrist position of the recorded data of the participants during the experiments, obtaining an error of less than 5 degrees. One year later, in [10], they used the same function to estimate the swivel angle, this time in combination with a viscoelastic muscle-like model of the arm, with a variable damping. With this approach, they obtained more accurate estimation of the swivel angle compared with the pure kinematic constrain estimation.

On the other hand, swivel angle estimation can be also estimated by learning from the synergies showed by humans performing specific activities. In [2], a non-linear function is proposed to estimate the swivel angle given a hand pose (position and orientation). For this study, kinematic data of healthy subjects was recorded with the used of a motion capture system. The subjects were asked to move their right hand palm around the surface of a rigid 7 cm radius sphere, this with the purpose of simulating assembling movements. First, this data was used to analyze the relation between the hand pose and the swivel angle. Then, after normalizing the data to a single arm lenght, a nonlinear function was obtained to calculate a swivel angle in function of the hand pose (x, y, z Cartesian coordinates, and ρ, θ, ϕ Euler

angles). The estimations of the proposed function were compared with the entire dataset, obtaining a root mean square (RMS) values of less than 9%.

All these studies show that the swivel angle is a good approach to resolve the kinematic redundancy of the arm in order to generate human-like trajectories in upper arm exoskeletons. Also, it was proved that it is possible to learn from the natural movements of people performing specific movements to create cost functions that could estimate a swivel angle considering the natural synergies contained in the kinematic data. It can be said that this is an efficient and simple approach, in comparison with other analytic and more complex solutions, where kinematic and muscle-like models need to be considered.

1.2 The ANYexo

The ANYexo is an upper-limb exoskeleton for rehabilitation of patients that have suffered a neural impairment, covering moderately to severe affected people. The device is based in a low-impedance torque controllable series elastic actuators (SEAs) [11], which opens the possibility for the device to serve as an experimental platform for testing novel control algorithms based on torque control for rehabilitation purposes. One of the features that this exoskeleton presumes, beside the high fidelity torque control, is a wide ROM that allows the user to perform activities of the daily living (ADLs), including movements close to the torso, head and behind the back.

Another remarkable feature of the ANYexo is its kinematic structure. It has a total of 9-DOF fulfilling the kinematic structure of the human arm. For the shoulder it considers the spherical joint of the Glenohumeral joint (GH), as well as the elevation/depression (GED) and the protraction/retraction (GPR) provided by the movement of the shoulder girdle (SG). These provide the first 5-DOF of the device. The next DOF is located at the elbow joint, followed by the 3-DOF spherical joint of the wrist.

This kinematic configuration resembles the kinematic chain presented in the human arm. This means that a kinematic redundancy will need to be resolved for the generation of human-like trajectories.

In the present work, the creation of a function for the estimation of optimal swivel angles for a given hand pose will be used to resolve the kinematic redundancy in the ANYexo with the purpose of generating motion profiles based in the synergies used by humans when performing daily tasks.

1.3 The U-LIMB database

The U-Limb database is a large, multi-modal, and multi-center data collection on human upper-limb movements. This was the result of the collaboration between six different institutions. In total, the database contains data from 91 able-bodied and 65 post-stroke participants. The data is organized by three types:

- Kinematic, electromyography, electroencephalography and electrocardiography signal from subjects performing ADLs using their upper limb.
- Force-kinematic behavior while the subject was performing precise manipulation tasks by interacting with a haptic device.
- Brain activity during hand control using functional magnetic resonance imaging.

Previous datasets present important information regarding the human locomotion. However, the U-Limb data set introduces an exhaustive collection of data with two great novelties: multi-modality and multicentricity, this means that information was collected at different research and clinical centers considering the same protocols. As well, this study considered the entire kinematic chain of the arm for the acquisition of the data, both from healthy and post-stroke participants. This data can help to analyze and know more about the workspace and phenomenological characteristics of upper limb movements from healthy participants and could be used evaluate the severity of the motor impairments of patients with reduce mobility.

The information provided by this dataset could help to have a better understating of the kinematic and dynamics of the human arm when performing activities of the daily life. This is valuable information that could be used to improve the design and control of assistive and rehabilitation robots, improving the human-machine interaction. One example of this is the work presented by Averta et. al [12], where the kinematic data of healthy subjects performing activities of the daily living was used to extract the principal motion patterns by using functional Principal Component Analysis (fPCA). In this way, they were able to reconstruct human upper limb trajectories by a linear combination of few principal time-dependent functions. This contribution allows to infer that complexity of the movement from the human arm can be reduce by modulating their motion through a reduced set of principal patterns. In this work, the kinematic data provided by this dataset will be used to find synergies of the elbow from healthy humans performing activities of the daily living.

1.4 Contribution

For this study, a correlation of the hand pose (position and orientation) with the swivel angle is hypothesized. Kinematic data from healthy subjects performing activities of the daily living is analyzed to compute the swivel angle together with its respective hand pose. As a result, a new database is created, working as "lookup table" from which the the swivel angle will be computed using a cost function which considers the orientation and position of the hand, being possible to assign different weight to each one of these parameters. The proposed cost function and database is intended to be implemented in the upper limb exoskeleton ANYexo to perform human-like trajectories during rehabilitation therapies.

2 Methodology

2.1 Analysis Pipeline

The main goal of this study if to generate a function that, considering the data from the healthy participants of the database, could compute the optimal elbow elevation angle for an specific position and orientation of the hand. The Figure 1 presents a general description of how this was achieved. First, the kinematic data of healthy subjects performing ADLs will be used to compute the swivel angle during the trajectories. This value is stored together with the hand pose of the subject at that specific frame. The same process was repeated for every trial, task and subject.

All this data will be stored in a database which will work as as 'lookup table' from which an optimal swivel angle will be computed using a cost function that will consider the desired hand pose (Cartesian coordinates and Euler rational angles). By iterating this process over the time for the trajectory of the hand, it can be obtained the optimal swivel angle of the arm during the movement. As motioned before, the estimation of a swivel angle will work a solution for the kinematic redundancy in arm exoskeletons.

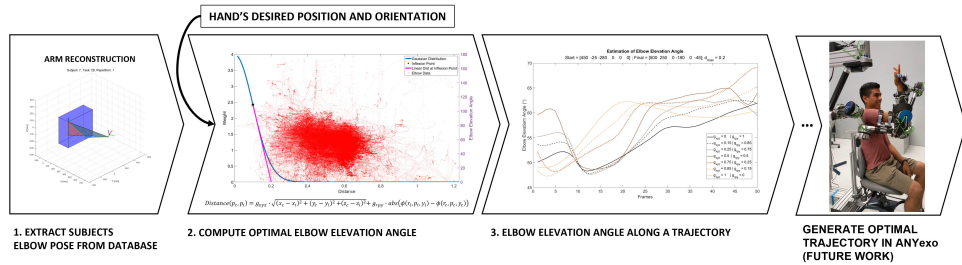


Figure 1: Pipeline for the estimation of optimal elbow elevation angle (swivel angle).

2.2 Kinematic Data

For this study, only the kinematic data provided by the University of Pisa (UP) with in the U-LIMB database was considered. In total, it contains data from 39 subject, performing 30 ADLs with three repetitions each one. This activities are described on detail on Table 1. The kinetic data was captured through a PhaseSpace motion capture system, placing active markers placed in rigid supports fastened to the subjects: 4 markers on the chest, 6 markers on the arm, 4 markers on the hand dorsum, and 20 markers on the fingers (4 for each finger). The arrangement of the markers is depicted in Figure 2. The data was sampled at a frequency of 100Hz. All of the participant were right handed.

ADL No.	Task Class	Description
1	Intransitive	Ok gesture (lifting hand from the table)
2		Thumb down (lifting hand from the table)
3		Exultation (extending the arm up in the air with closed fist)
4		Hitchhiking (extending the arm along the frontal plane, laterally, parallel to the floor, with extended elbow, closed fist, extended thumb)
5		Block out sun from own face (touching the face with the palm and covering the eyes)
6		Greet (with open hand, moving wrist) (3 times)
7		Military salute (with lifted elbow)
8		Stop gesture (extending the arm along the sagittal plane, parallel to the floor, open palm)
9		Pointing (with index finger) at something straight ahead (with outstretched arm)
10		Silence gesture (bringing the index finger, with the remainder of the hand closed, to the lips)
11	Transitive	Reach and grasp a small suitcase by the handle, lift it, and place it on the floor (close to own chair, along own sagittal plane)
12		Reach and grasp a glass, drink for 3 seconds, and replace it in the initial position
13		Reach and grasp a phone receiver, carry it to own ear and hold for 3 seconds, and replace it in the initial position
14		Reach and grasp a book (placed overhead on a shelf), put it on the table, and open it (from right side to left side)
15		Reach and grasp a small cup by the handle (2 fingers + thumb), drink for 3 seconds, and replace it in the initial position
16		Reach and grasp an apple, mimic biting, and replace it in the initial position
17		Reach and grasp a hat by its top and place it on own head
18		Reach and grasp a cup by its top, lift it, and put it on the left side of the table
19		Receive a tray (straight ahead, with open hand) and put it in the middle of the table
20		Reach and grasp a key in a lock (vertical axis), extract it from the lock, and put it on the left side of the table
21	Tool-mediated	Reach and grasp a bottle, pour water into a glass, and replace the bottle in the initial position
22		Reach and grasp a tennis racket (placed along own frontal plane) and play a forehand (the participant is still seated)
23		Reach and grasp a toothbrush, brush teeth (horizontal axis, 1 time left-right), and put it inside a holder (on the right side of the table)
24		Reach and grasp a laptop, open it (without changing its position) (4 fingers + thumb)
25		Reach and grasp a pen (placed on the right side of the table) and draw a vertical line on the table (from the top to the bottom)
26		Reach and grasp a pencil (placed along own frontal plane) (3 fingers + thumb) and put it inside a square pencil holder (placed on the left side of the table)
27		Reach and grasp a tea bag in a cup (1 finger + thumb), remove it from the cup, and place it on the table on the right side of the table
28		Reach and grasp a doorknob, turn it clockwise and counterclockwise, and open the door
29		Reach and grasp a tennis ball (with fingertips) and place it in a basket on the floor (right)
30		Reach and grasp a cap (2 fingers + thumb) of a bottle (held by left hand), unscrew it, and place it overhead on a shelf

Table 1: List of activities or daily living (ADL) performed by the subjects [1]

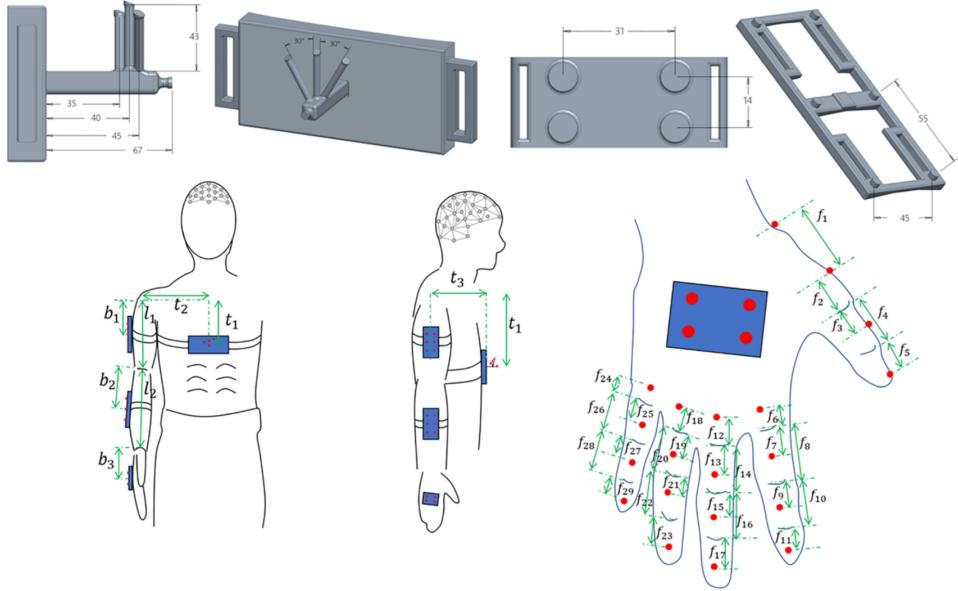


Figure 2: Anatomical placement of active markers, and details on the marker support used for the experiments at UP. Numerical values on the dimensions of marker support are reported in millimeters [1]

2.2.1 Data filtering

Considerable noise was observed in the spacial data (XYZ coordinates) of the markers. Since this data was planned to be used for the calculation of the swivel angle, removing the noise from the kinematic data was desired. For this, a median filter was applied to all the marker's kinematic data. The median filter considered the first 4 surrounding points.

Also, since the analyzed data was to be analyzed in a statistical manner, only data of the subject in movement was to be considered for the generation of the database. To remove data of the subject during static poses, the start and end of the movement was based in the velocity profile of the hand. This because all the ADLs were reaching based tasks. A velocity above 5mm/s on the hand's dorsum markers was considered the start of the movement, while a velocity below this same value was considered as the end of the movement.

2.2.2 Redefinition of the world coordinates

The XYZ values from the kinematic database was rearranged so it be coincident with the world reference frame used in the ANYexo. The x axis points toward the front of the user, the y axis would be oriented to the left hand side, while the z would be pointing towards the ceiling.

2.3 Arm reconstruction

The swivel angle, as described in the previous section, is the angle that goes around a vector starting from the shoulder to the wrist joint. This angle, which can be referred as the elbow elevation angle, is obtained by measuring the angle between two planes: the first one formed by the shoulder-elbow-wrist joints, as the second plane is formed by the shoulder-wrist joints

together with a point along the z axis in the negative direction. The Figure 3 presents an illustration of how the swivel angle is measured between these planes.

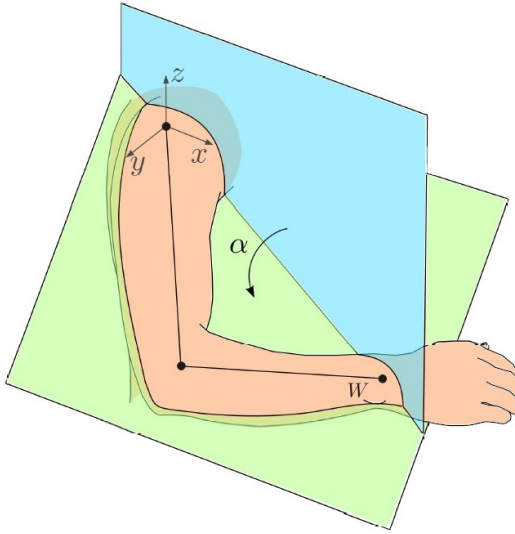


Figure 3: Definition of the swivel angle [2]

As it can be visualized in Figure 2, no markers were placed in the anatomical joints of the arm. In order to create the planes for the measurement of the swivel angle, the shoulder, elbow, and wrist joints need to be estimated from the kinematic data that is available.

To achieve this, the markers cluster placed on the arms, forearms and hand were used to obtain the orientation of these arm links. As it can be observed in Figure 2, the supports used to hold the markers can be considered as a two parallel series of markers. In the case of the arm and the forearm, two vectors were estimated using a linear regression, considering the three markers on the right, named v_1 , and the other three markers on the lefts, named v_2 . This description is true considering the illustration showed in Figure 2. Then, the orientation of the arms and forearm were obtained by computing the average of vectors v_1 and v_2 .

For the hand, a similar approach was taken. In this case, v_1 and v_2 were obtained merely by considering the two markers on each side of the support. Again, the average of these two vectors was considered as the orientation of the subject's hand. The reference frame for the hand ($X_h Y_h Z_h$) was placed in the center of the markers placed in the hand's dorsum. The same vector that was considered as the hand's orientation was given to the X_h axis. A cross product was made between the X_h and vector formed by two of the markers from the hand cluster, resulting in a orthogonal vector which was assigned to the Z_h axis. Finally, the Y_h axis was obtained by the cross product $\vec{Z}_h \times \vec{X}_h$. The average vectors computed for the arm, forearm and hand were named v_a , v_{fa} and v_h , respectively, depicted in Figure 4.

By using the equation $v_u = v / \|v\|$, the unit vector for each one of the links of the arm was calculated. Let v_{uh} , v_{ufa} and v_{ua} represent the unit vector for the hand, forearm and arm, respectively. This unitary vectors contain the orientation data of its respective arm link at a specific frame. The UP data set provided anatomical measurements of every participant. In

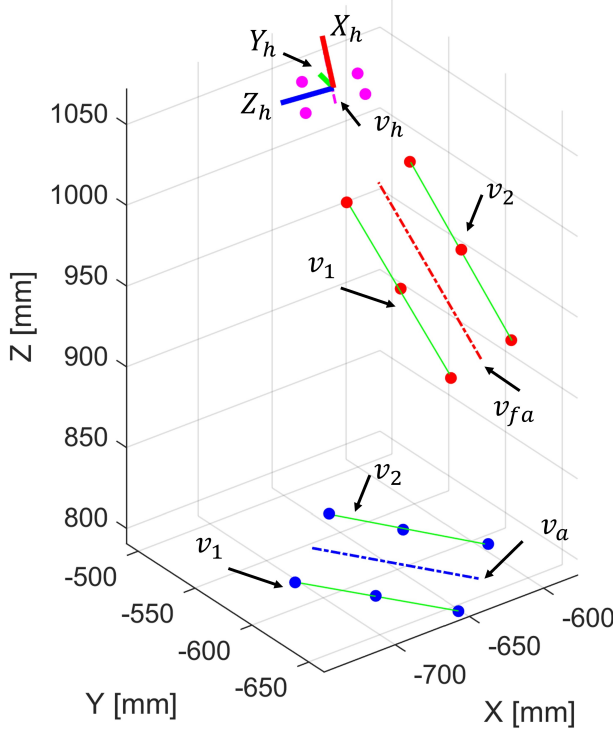


Figure 4: Visualization of the vector v_a , v_{fa} and v_h obtained from the marker's data.

Figure 2, the measures l_1 , l_2 and b_3 correspond to the length of the arm, forearm, and wrist to center of the hand, respectively. Considering these measures, together with the unit vector calculated from the marker's data, it was possible to create a reconstruction of the subject's arm at every frame.

To start, the world reference frame (WRF) XYZ of every subject was set at the shoulder, using the same orientation as the ANYexo's reference frame. Then, the unit vector v_{ua} of the arm was multiplied by its corresponding length l_1 , resulting in a vector that corresponds to the arm link. The unit vector v_{ufa} multiplied by l_2 projecting a vector representing the forearm link. Finally, v_{uh} multiplied by b_3 gave as result a vector which was assumed started from the wrist to the center of the hand. These vectors were arranged sequentially to create a reconstruction of the subject's arm. The illustration provided in Figure 5 shows the result of the aforementioned procedure, where the blue box represents the torso of the subject, the green lines are the arm links, as the blue dots correspond to the shoulder, elbow, wrist, and center of the hand joints. It was hypothesized that the elbow joint was placed at the intersection of the obtained arm and forearm links, whereas the wrist joint was located at the end of the forearm link. Also, Figure 5 shows the placement of the world reference frame at the subject's shoulder, while the hand's reference frame (HRF) is placed at the last joint of the arm that corresponds to the center of the hand, showing the actual orientation and position of it.

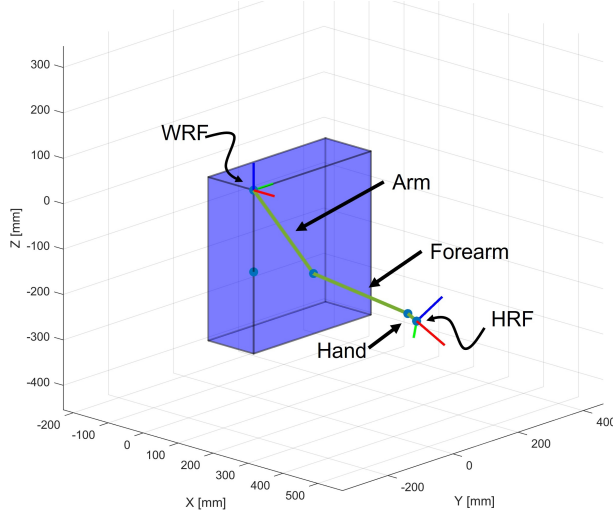


Figure 5: Example of a subject's arm reconstructions. World reference frame (WRF) place at the shoulder, and hand's reference frame (HRF) placed at the center of the hand.

2.4 Elbow elevation angle

Once the arm of the subject that been reconstructed, the shoulder, elbow and wrist joints Cartesian coordinates can be obtained. The shoulder, placed a the origin of the WRF, has a position of $[0, 0, 0]$. The position of the elbow is considered as the end point of the vector that correspond to the arm link. Finally the wrist joint is taken as the end point of the forearm vector. Having the Cartesian coordinates of the these joints it is possible to create the planes that will be used to measure the swivel angle, i.e. the elevation angle of the elbow. Let p_1 be a plane formed by a vector v_{nz} pointing in the negative z direction of the WRF, and a vector v_{sw} which starts from the shoulder to the wrist joint. Then, let p_2 be a plane formed by the same previous vector v_{sw} , and a vector v_{se} which will start from the shoulder to the elbow joint.

The swivel angle was obtained by the following equation:

$$\alpha = 180^\circ - \arccos\left(\frac{\hat{v}_{p1} \cdot \hat{v}_{p2}}{\|\hat{v}_{p1}\| * \|\hat{v}_{p2}\|}\right) \quad (1)$$

Where α represents the swivel angle. The unitary vectors \hat{v}_{p1} and \hat{v}_{p2} are obtained from vectors v_{p1} and v_{p2} , which are normal vectors to planes p_1 and p_2 , respectively. The normal vector v_{p1} is obtained by the cross product $v_{nz} \times v_{sw}$, whereas v_{p2} by $v_{sw} \times v_{se}$. In this manner, the elbow elevation angle can be computed at every pose the subject performed during the data collection.

2.5 Axis Rotation Angle

The proposed cost function for the estimation of the optimal swivel angle has an specific hand pose as an input, considering the position and orientation of this. The $[x, y, z]$ Cartesian position of the subject's hand can be extracted from the kinematic data, through the arm reconstruction process aforementioned. In Figure 5, it is observed that the HRF is placed

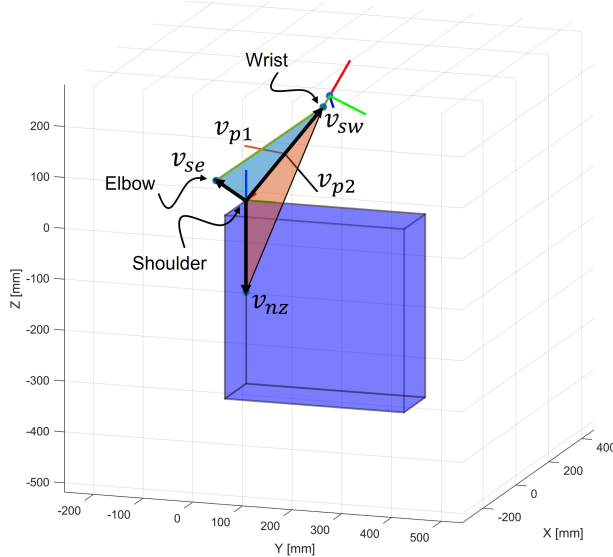


Figure 6: Vector v_{nz} and v_{sw} form the plane p_1 , and vector v_{sw} and v_{se} form the plane p_2 . Angle between planes p_1 and p_2 form the swivel angle.

at the center of the hand. The unit vectors X_h, Y_h, Z_h contain the data that describe the orientation of the the hand W.r.t. the WRF placed at the shoulder of the subject.

A single-axis rotation angle representation was used to describe the amount of rotation that a subject performed w.r.t. to the WRF at a specific position in the space. The single-axis rotation is one of the many representations used to describe a three dimensional rotation [13]. In comparison with a rotation Matrix, this representation uses two values to describe the rotation of a object in the space. The first value is a unit vector known as rotation vector, which is the axis the object is rotates around. The second value is the rotation angle ϕ , which is the amount of rotation around the rotation vector. For the generation of the dataset, only the magnitude of ϕ was obtained from the kinematic data of the subject.

A rotation matrix is formed by arranging the unit vectors from the HRF as follows:

$$\begin{bmatrix} Xh_x & Yh_x & Zh_x \\ Xh_y & Yh_y & Zh_y \\ Xh_z & Yh_z & Zh_z \end{bmatrix} \quad (2)$$

In which the $[x, y, z]$ components of the X_h, Y_h, Z_h unit vectors from the HRW, are arranged in the first, second and third rows, respectively. This same matrix was used to compute the axis rotation angle ρ by the equation::

$$\rho = \arccos \left\{ \frac{1}{2} \left(Xh_x + Yh_y + Zh_z - 1 \right) \right\} \quad (3)$$

The function `rotm2eul` was used for the implementation of this process in MATLAB.

Also, the orientation of the hand was calculate in the Euler rotation angle representation. In equations (4)(5)(6), the Euler rotation angles are obtained using the same rotation matrix in (2). The variables θ, ψ, ϕ correspond to the Euler rotation angles Roll, Pitch and Yaw,

Swivel Angle	X	Y	Z	Roll	Pitch	Yaw	Axis Rotation Angle
1	1	1	1	1	1	1	1
:	:	:	:	:	:	:	:
n	n	n	n	n	n	n	n

Table 2: Format of stored processed data for each subject.

respectively [14].

$$\theta = \arccos(Zh_z) \quad (4)$$

$$\psi = \arctan\left(\frac{Zh_y}{Zh_x}\right) \quad (5)$$

$$\phi = \arctan\left(\frac{Yh_z}{-Xh_z}\right) \quad (6)$$

In MATLAB, the function `rotm2eul` can be used to obtain the Euler rotational angles given a rotation matrix.

2.6 Swivel angle database

The estimation of an optimal swivel angle will be based in the movements performed by healthy subjects when performing ADLs. The elbow elevation angles from the subjects will be extracted from the kinematic data collected by the UP.

All the kinematic data available in the data set will be processed. A total of 3,510 files containing the motion capture data of all the 39 subjects, performing the 30 ADLs with a total of 3 repetitions each. These data was processed using MATLAB scripts. Every file was processed frame by frame, extracting the swivel angle together with its respective hand pose (Cartesian coordinates, Euler angles, and axis rotation angle). For each subject, a '.mat' file was created. This file contained a cell array, dividing each ADL by columns, and the repetitions in its respective row, resulting is a matrix of 3×30 . Each cell from this matrix contains data arranged in the format showed on Table 2, where each row correspond to the data of a 'n' frame. In this manner, 39 datasets were created, one for each subject, storing the data regarding the swivel angel and hand pose performed along all the trials.

2.6.1 Clustering data by arm length

Since this databases will serve as 'lookup tables' to estimate the elbow angle, it was decided to group the databases according to the arm length of the subjects. It is hypothesized that the arm length of the subjects influence in the swivel angle considered optimal for that specific subject. The arm length of the subjects was obtained by adding up the variables l_1 , l_2 and b_3 , corresponding to the anatomical measures of the arm link from each subject. These data which was provided within the UP database (Figure 2).

Figure 7 shows an histogram with the arm length distribution of the 39 participants from the UP database. The histogram shows eighth groups. The length range for each group can be observed in Figure 7. These ranges were considered to cluster the datasets of the subjects according to their arm length. As a result, eight cluster were created, saved as '.mat' files. Each one of these files contains the same data and format showed in Table 2, adding a ninth column containing the number of the respective ADL (see Table 1). In comparison with the datasets per subject, were data was stored in cell arrays per tasks as repetition, these clusters contained all the data (all the frames, from every repetition, task and subject) in a single table. In this manner, the computational cost would be reduced when running the cost function through all the data contained in these clusters.

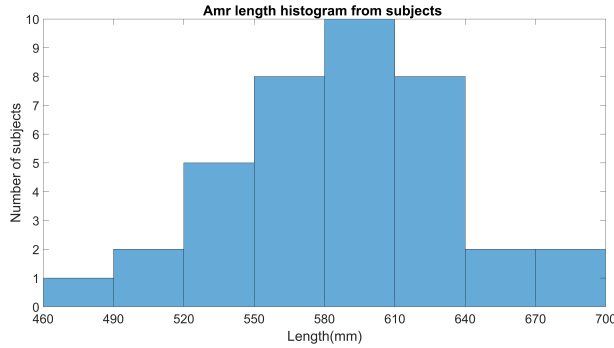


Figure 7: Arm length histogram of the 39 participants from the UP database.

2.7 Cost function for estimation of swivel angle

A cost function is proposed to estimate an optimal swivel angle given an arbitrary hand pose. This pose will consist of a 6-dimensional pose p_c , describing the position and orientation of the hand in the space.

$$p_c = \begin{pmatrix} x \\ y \\ z \\ \theta \\ \psi \\ \phi \end{pmatrix} \quad (7)$$

Were $[x, y, z]$ correspond of the Cartesian coordinates, and $[\theta, \psi, \phi]$ represent the Euler rotation angles. This would be an specific hand pose a given a time step t .

By processing the kinematic data from the subjects, it is possible to know the elbow elevation angle ELB_i at any given pose p_i performed by the participants during the trials.

$$ELB_i = g(p_i) \quad (8)$$

Ultimately, it is desired to find a function ELB_c that calculates the elbow elevation angle for an arbitrary pose p_c :

$$ELB_c = f(p_c) \quad (9)$$

where

$$f(p_c) = \frac{\sum_{i=1}^N w(p_c, p_i) \cdot g(p_i)}{|\sum_{i=1}^N w(p_c, p_i)|} \quad (10)$$

will estimate the elbow elevation angle along a trajectory, conformed by a series of p_c desired poses. Here, for the estimation of the elbow elevation angle, a weighting function is used:

$$w(p_c, p_i) = \frac{1}{\sigma\sqrt{2\pi}} e^{\left(\frac{-(d(p_c, p_i))^2}{2\sigma^2}\right)} \quad (11)$$

in which $d(p_c, p_i)$ is a distance, i.e. it is 0 if $p_c = p_i$, and > 0 otherwise. A Gaussian distribution function will assign a weight value to the given distance $d(p_c, p_i)$, considering a $\mu = 0$ and a given standard deviation σ . The method to obtain σ will be explained in brief.

The distance function to implement is:

$$d(p_c, p_i) = \varrho \sqrt{(x_c - x_i)^2 + (y_c - y_i)^2 + (z_c - z_i)^2} + (1 - \varrho) \cdot \text{abs}(\rho(\theta_i, \psi_i, \phi_i) - \rho(\theta_c, \psi_c, \phi_c)) \quad (12)$$

where $\rho(\theta_i, \psi_i, \phi_i)$ is the axis rotation angle in function of the Euler angles given a desired hand orientation w.r.t. the WRF. The variable ϱ is a weighting parameter that will give more relevance either to the Cartesian position or to the orientation when estimating the optimal swivel angle for the desired hand pose.

2.8 Standard deviation based in a maximum distance

Consider the function of a Gaussian distribution:

$$f(x) = \frac{1}{\sigma\sqrt{2\pi}} e^{\left(\frac{-x^2}{2\sigma^2}\right)} \quad (13)$$

and its derivative:

$$f'(x) = \frac{-x}{\sigma^3\sqrt{2\pi}} e^{\left(\frac{-x^2}{2\sigma^2}\right)} \quad (14)$$

the inflexion point of a Gaussian distribution occurs when $f(x)$ is evaluated in σ . It is desired to merge the Gaussian distribution curve with a straight line, such slope be that

$y(0) = d_{max}$. In this manner, the slope can be equaled to the derivative of the Gaussian distribution evaluated at the inflexion point σ . This can be expressed as:

$$\frac{f(\sigma)}{d_{max} - \sigma} = f'(\sigma) \quad (15)$$

Considering $x = \sigma$ and $\mu = 0$ in equations (13) and (14), the equation (15) can be expressed as follows:

$$\frac{\frac{1}{\sigma\sqrt{2\pi}}e^{\left(\frac{-\sigma^2}{2\sigma^2}\right)}}{d_{max} - \sigma} = \frac{-x}{\sigma^3\sqrt{2\pi}}e^{\left(\frac{-\sigma^2}{2\sigma^2}\right)} \quad (16)$$

Where σ would we:

$$\sigma = \frac{d_{max}}{2} \quad (17)$$

3 Results

3.1 Evaluating distance function

A optimal swivel angle is desired to be obtained given an arbitrary hand pose using the function expressed in (10). This function will make use the clusters described in previous section, containing data regarding the elbow elevation angle of the participants when performing ADLs. For this, the arm length of the subject for which the function will be evaluated need to be declared.

The first step it to define the six-dimensional desired hand pose p_c , which will be the input to be evaluated in the distance function (12). For this, the weighting parameter ϱ also needs to be defined, to determined the relevance of the Cartesian position and orientation. The output of this function will be considered as the similarity of the desired hand pose p_c in comparison with a hand pose p_i from the database. Here, the magnitude of the output will be proportional to the difference of the p_c w.r.t. p_i . A value of 0 is expected whenever $p_c = p_i$, and > 0 otherwise.

The function compares the desired hand pose with all the hand poses stored in the respective dataset cluster. As a result, a vector is generated, containing the distance of p_c w.r.t all the p_i . Figure 8 show the result of plotting all the distances $d(p_c, p_i)$ with its respective swivel angle $g(p_i)$. The distance values are plotted along the x axis, whereas the y axis displays the respective swivel angle p_i . Remarking that the values closer to a distance equal to 0, have a higher similarity. Following this logic, the respective swivel angles represent a possible solution for the given hand pose. The color and type of the markers correspond to an specific ADL. By observing this plot, it can be noticed that some specific ADLs contain hand poses with a higher similarity when compared with the desired one. However, the statistical approach

used to compute an optimal swivel angle did not give higher relevance to those specific ADLs.

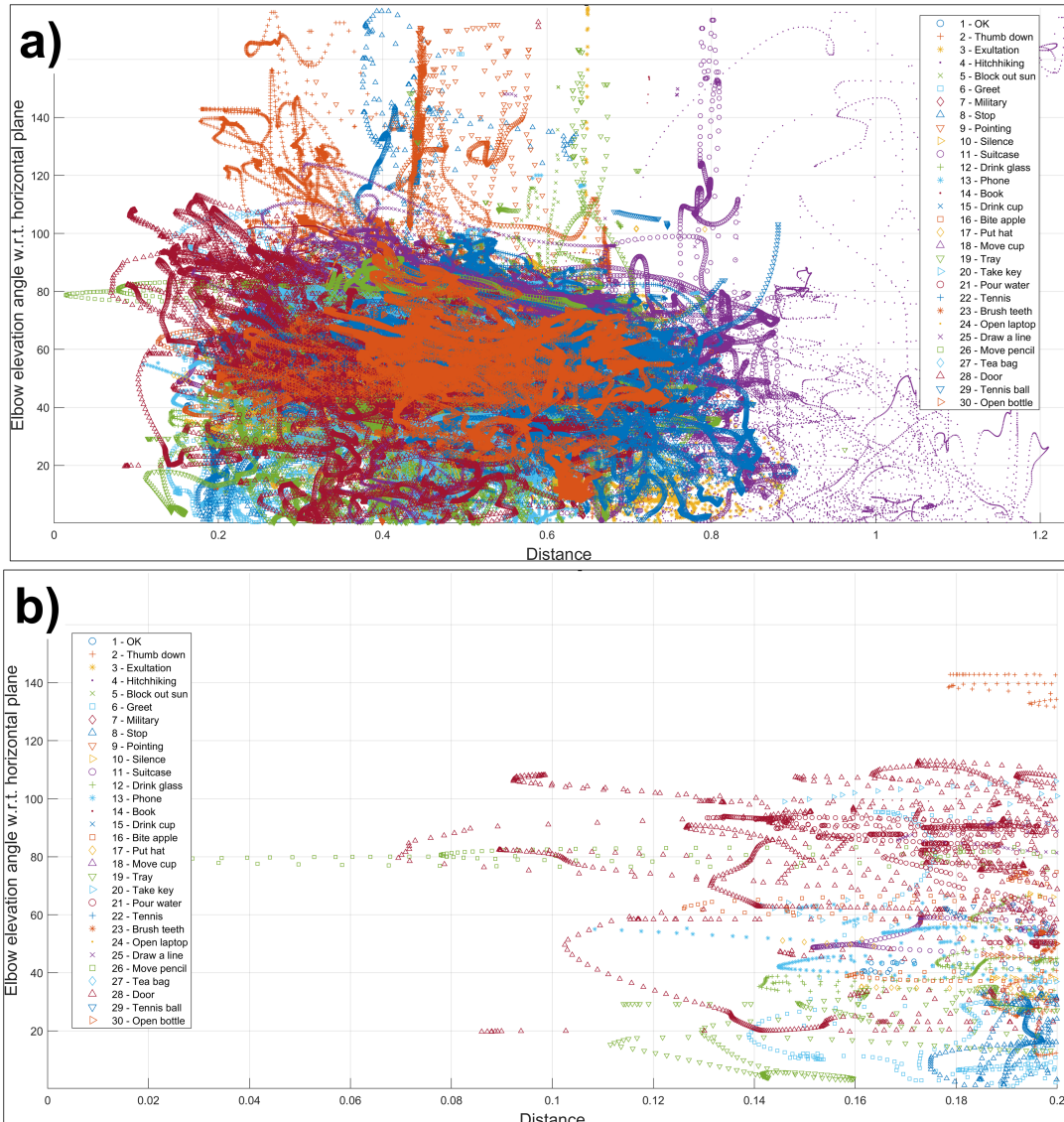


Figure 8: **a)** Scatter plot showing the distance function evaluated at the desired hand pose. ADLs identified by color and marker type. **b)** Scatter plot only displaying values below the maximum tolerated distance d_{max}

3.2 Gaussian distribution of distance data

As showed in figure 8, more than a one swivel angle present a higher similarity given a desired hand pose. For this reason, the approach in the proposed equation (10) is to obtain an average of all the possible swivel angles multiplied by its respective weight magnitude. This weight if obtained by the equation (11), where a Gaussian distribution function is used to obtain the weight (or relevance) of an specific swivel angle according to its position in the normal distribution of the distances obtained by evaluating the distance function $d(p_c, p_i)$ at the given hand pose.

The standard deviation σ of the Gaussian distribution is obtained in function of a maximum distance magnitude d_{max} . Once d_{max} is defined, σ is obtained by the function (17). The value of σ will define the distribution of the Gaussian function. By evaluating $f(\sigma)$, the inflexion point of the curve is found, and the values of the normal distribution above this point are replaced by a linear function $y(x)$ starting from the inflexion point. The slope of $y(x)$ being equal to $f'(\sigma)$, so $y(0) = d_{max}$. An example of the resulting Gaussian distribution in combination with the linear function is depicted in Figure 9. The Gaussian distribution (blue line) showed in the example was generated from the same data showed in Figure 8. Here the value of σ was obtained by setting a $d_{max} = 0.2$. In Figure 9, the resulting linear function $y(x)$ is displayed in magenta. It can be observed that the valued of $y(0)$ is equal to the d_{max} that was established. A $\rho = 0.5$ was considered when evaluating the function $d(p_c, p_i)$, giving equal weight for both the Cartesian position and orientation of the desired hand pose.

This resulting distribution contains the weights that will be assigned to each one the of the swivel angles with a distance $d(p_c, p_i)$ below the d_{max} threshold. Having these values, its possible to evaluate the cost function $f(p_c)$. For the showed example, the desired hand pose was set as $p_c = [500, 250, 0, -180^\circ, 0^\circ, -45^\circ]$, at this position the hand would be placed in front of the subject a the level of the shoulder like doing a 'thumb down' pose. Given this pose, the function $f(p_c)$ estimated a swivel angle $\alpha = 64.0348^\circ$.

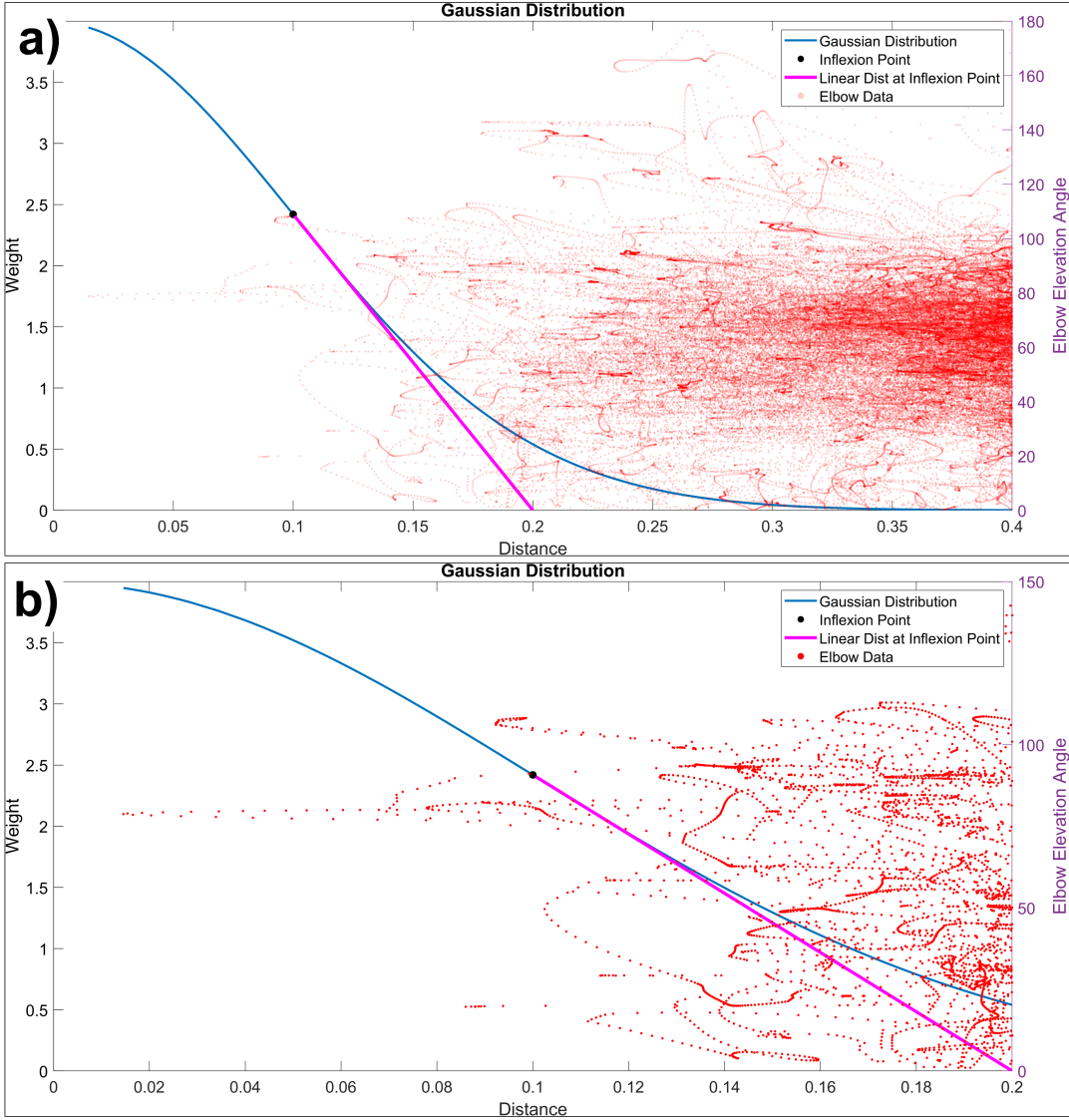


Figure 9: **a)** Gaussian distribution in combination with a straight line starting at the inflection point of the curve. **b)** Data points below the d_{max} threshold.

3.3 Swivel angle along a trajectory

The example in the previous subsection demonstrated the procedure to compute the required data to evaluate the cost function (10) and obtained an estimated swivel angle given an arbitrary hand pose. This same process can be iterated in time using a progressive hand pose and thus, estimate the variation of the swivel angle along such trajectory.

For this, the cost function (10) is evaluated along a trajectory to obtain the swivel angle progression. To generate the trajectory, a linear interpolation was made between an start and end hand poses. In the following figures, 50 position were interpolated from the initial and final pose. Each one of the examples depicted in the following figures show three different plots. The same movement was evaluated using a different d_{max} tolerated distance: 0.15, 0.2, and 0.25. Also, five different magnitudes of the weighting parameter ρ were used in each one of the scenarios. By comparing the results when using a different ρ , it is possible to observe

the effect in the swivel angle estimation when giving more relevance either to the Cartesian position or orientation of the desired hand pose. The 'subject' for which the trajectories were going to be generated was given an arm length of 620 mm. With this arm length, the dataset cluster within the arm length range of 610 – 640 mm was used to estimates the optimal swivel angles. This dataset is the second one with most data available.

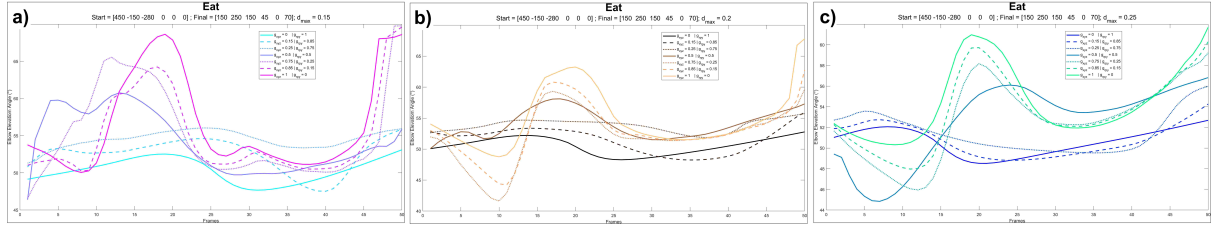


Figure 10: Swivel angle progression for a movement mimicking the action of taking food to the mouth. **a)** $d_{max} = 0.15$. **b)** $d_{max} = 0.2$. **c)** $d_{max} = 0.25$.

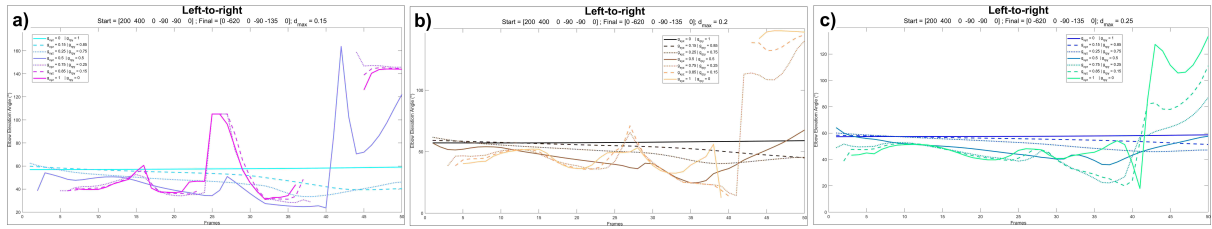


Figure 11: Swivel angle progression for a movement mimicking the action of moving the hand from left to right side at the shoulder level. **a)** $d_{max} = 0.15$. **b)** $d_{max} = 0.2$. **c)** $d_{max} = 0.25$.

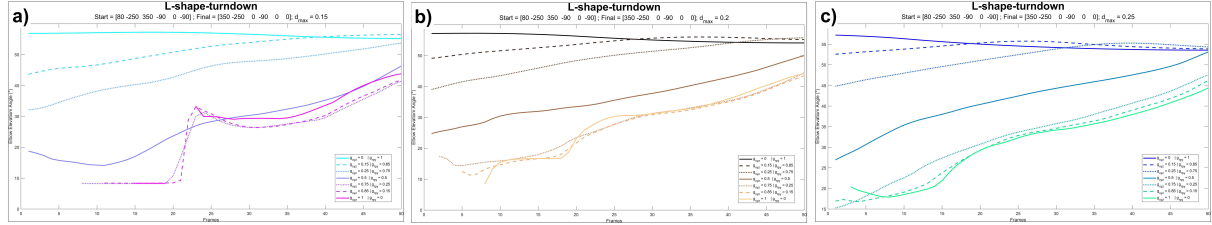


Figure 12: Swivel angle progression for a movement mimicking the action of placing the hand on the right side, fingers pointing upwards and arm forming and 'L' shape, turning the arm until the palm face downwards. **a)** $d_{max} = 0.15$. **b)** $d_{max} = 0.2$. **c)** $d_{max} = 0.25$.

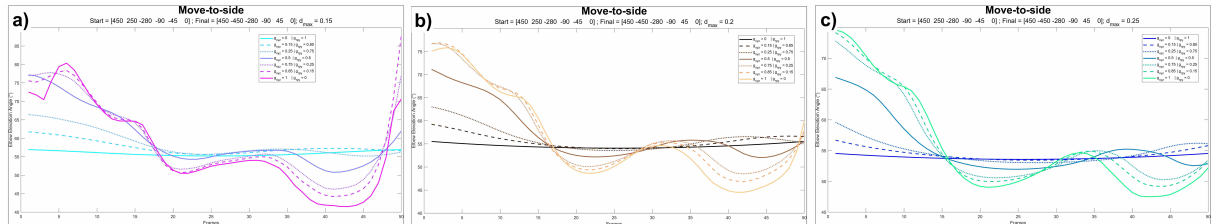


Figure 13: Swivel angle progression for a movement mimicking the action of displacing the hand from right to left along a surface below the shoulder level. **a)** $d_{max} = 0.15$. **b)** $d_{max} = 0.2$. **c)** $d_{max} = 0.25$.

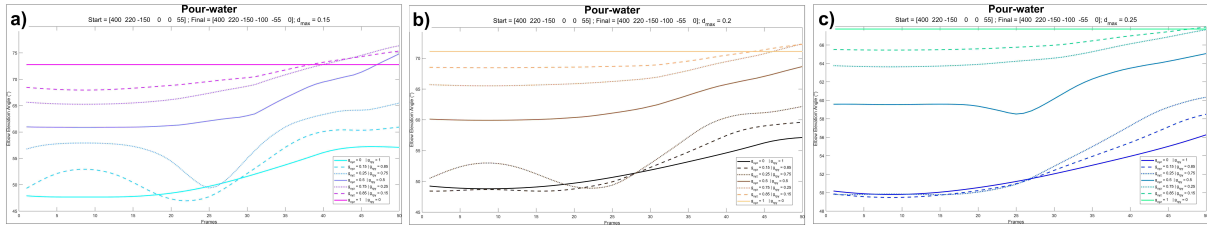


Figure 14: Swivel angle progression for a movement mimicking the action of pouting water into a container place on a table in front of the subject. **a)** $d_{max} = 0.15$. **b)** $d_{max} = 0.2$. **c)** $d_{max} = 0.25$.

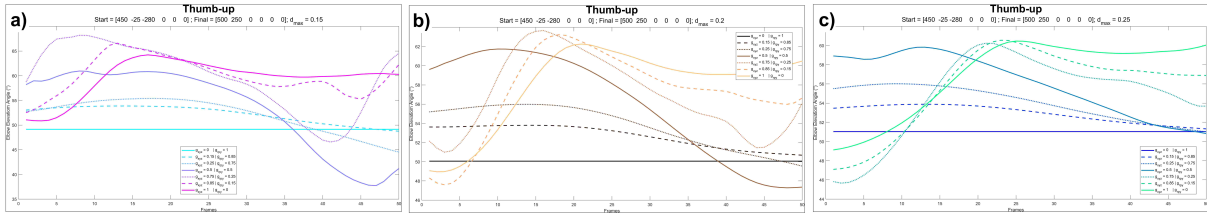


Figure 15: Swivel angle progression for a movement mimicking the action of a 'thumb up' expression, placing the hand in front of the subject. **a)** $d_{max} = 0.15$. **b)** $d_{max} = 0.2$. **c)** $d_{max} = 0.25$.

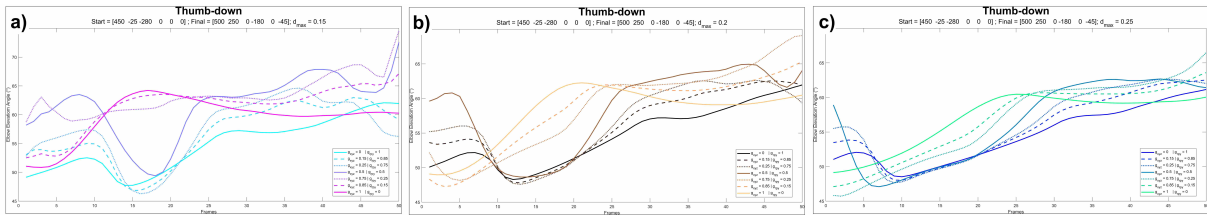


Figure 16: Swivel angle progression for a movement mimicking the action of a 'thumb down' expression, placing the hand in front of the subject. **a)** $d_{max} = 0.15$. **b)** $d_{max} = 0.2$. **c)** $d_{max} = 0.25$.

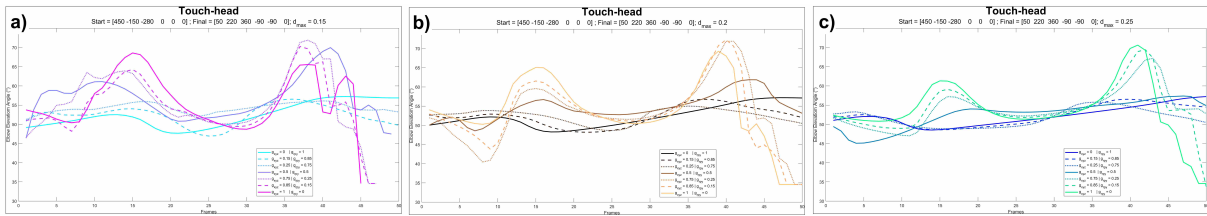


Figure 17: Swivel angle progression for a movement mimicking the action of reaching the top of the head with the palm. **a)** $d_{max} = 0.15$. **b)** $d_{max} = 0.2$. **c)** $d_{max} = 0.25$.

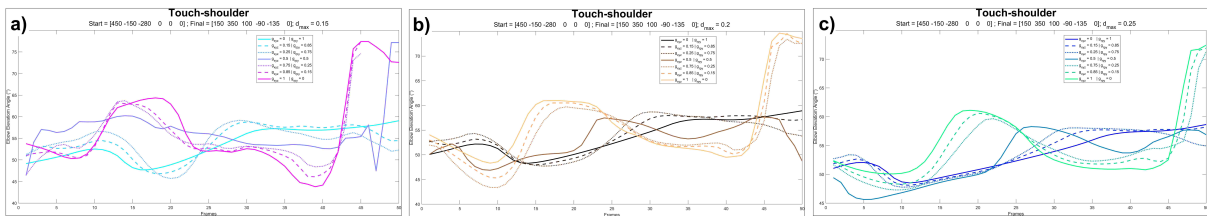


Figure 18: Swivel angle progression for a movement mimicking the action of reaching the left shoulder with the finger tips. **a)** $d_{max} = 0.15$. **b)** $d_{max} = 0.2$. **c)** $d_{max} = 0.25$.

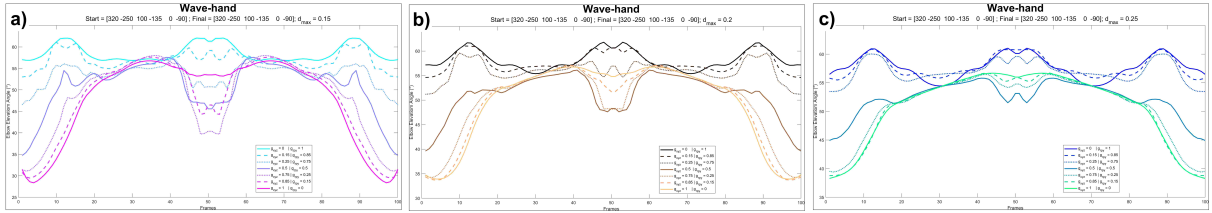


Figure 19: Swivel angle progression for a movement mimicking the action of waving the hand at the same position, only moving the wrist joint. **a)** $d_{max} = 0.15$. **b)** $d_{max} = 0.2$. **c)** $d_{max} = 0.25$.

4 Discussion

4.1 Interpretation of results

The efficacy of the proposed cost function to estimate an optimal swivel angle given a hand pose was tested by iterating the function in a sequence of hand poses that led to a trajectory. The outcomes of this function are showed from Figure 10 to 19. Here, the results will be analyzed and discussed.

First of all, with the proposed approach it was possible to compute elbow elevation angles all along the input trajectories. In most of the scenarios, the progression of the swivel angle was continuous and smooth. However, in the scenario showed in Figure 11, where trajectory consisted in moving the hand from the right side to the left shoulder, the progression of the swivel angle presents blank spaces and sudden peaks. This may be caused due to the lack of data regarding the swivel angle for some of the hand poses that were part of the trajectory. The same behaviour can be observed in Figure 12.

Another important factor to discuss is the influence of the weighting factor ρ in the estimation of the optimal swivel angle. The magnitude of ρ is proportional to the relevance given to the Cartesian coordinate component of the distance function. On the other hand, the relevance given to the orientation is define by $(1 - \rho)$. Thus, the lower ρ be, the higher relevance of the orientation component in the estimation of the optimal swivel angle for the given hand pose. Analyzing the results of the trajectories used for testing the proposed cost function, the influence of ρ can be noticed. producing significant changes in the progression of the elbow elevation angle in some scenarios. From all the trajectories, the ones in which the hand rotated around a single axis from the start to the end position, the swivel angle showed small, or even null, changes in the values of the swivel along the movement when the orientation component of the distance function had a higher relevance. On these scenarios, giving a higher weight to the Cartesian position component produced more variation in the estimated swivel angles. This phenomenon can be observed in Figures 11, 12, 13, 14 and 15. On the other hand, when the hand rotate around more than one axis during the movement, both the Cartesian positions and orientation components produce variation in the swivel angel along the trajectory. In these cases, a common pattern that can be identified is that

a higher variation of the swivel angle along is presented when more relevance is given to the Cartesian position component. This variation is more noticeable comparing the elbow elevation angle at the beginning and end of the movement.

Finally, the only impact of reducing the values of d_{max} is leading to no convergence in the estimation the swivel angle. This is caused by the shortening the amount of data to be considered in the cost function. When the desired hand position has very small similarity with the data available in the database, and all the possible swivel angles have a distance above d_{max} , it is not possible to compute a solution for that specific hand pose.

4.2 Limitations and improvements

One of the main drawbacks of the kinematic data used to create the database, is the present of noise and occlusion of the markers during the trials. Also, the range of movement covered by the ADLs performed by the participants in the study does not provide enough data for estimation of the swivel angle at the entire ROM of the human arm.

Several improvements can be made to the solution proposed in this work. One of them can be the identification of ADLs with a higher similarity with the desired hand pose, and consider only the data of those activities to estimate the swivel angle. Also, other statistical approaches can be used to assign specific weights to the possible elevation angles, instead of a Gaussian distribution. The weighting parameter ρ is another aspect that can be improved, by adjusting its value in function of the trajectory type.

Finally, the computational cost of this approach need to be optimized. The time required to compute a solution is around 0.09 s. If this approach is to be applied online in an exoskeleton, the algorithm needs to be at least ten times faster. Since the presented solution was implemented in MATLAB, one way of optimizing this solution may by the migration of the code to C++, and using a more efficient way to read the data from the data base.

5 Conclusion

Nowadays, robotics has achieved a high degree of development. This technology has found to be useful in more challenging applications, such is the case of rehabilitation. The use of exoskeletons for rehabilitation of upper limbs have gained interest, since it has proved to increase the efficiency of rehabilitation therapies [3]. However, by replicating the kinematic chain of the human arm, these robots also present a kinematic redundancy due to the high number of DOF. The use of the swivel angle has been a common approach in the literature for the solution of this kinematic redundancy. A database of kinematic data collected by the UP was analyzed to extract the swivel angle of healthy subjects performing several ADLs. The extracted data was used to create a new dataset, which serve as 'look up' table. A cost function was proposed, which, given an arbitrary hand pose, an optimal swivel angle is computed

taking as reference the data stored in the created database. Also, this function includes a weighting parameter to specify the relevance of the Cartesian coordinates and orientation of the desired hand pose for the estimation of the swivel angle. The function was evaluated in a set of different movements, determined by the desired trajectory of the hand. Analyzing the results, it was proved that the proposed function was able to estimate, in most of the cases, a continuous and smooth estimation of the swivel angle all along the trajectory. In some scenarios it was not possible to obtain a solution for specific hand poses, showing the lack of elbow data at some regions inside the ROM of the human arm. As well, the position and orientation of the hand influence in a significant manner the estimation a swivel angle.

The results of the proposed function still need to be improved, optimized and validated, by comparing the results with real human movements data. All of these need to be done before being implemented in an exoskeleton. More variables that are known to influence in the arm pose could also be included to improve the proposed approach. Variables such as physical restriction if the subject, force and direction of the movements, as well as biomechanic modelling of the human arm. Overall, the obtained results showed the possibility of estimating a swivel angle in function of the hand pose, based in kinematic data of healthy subjects. These opens the possibility to solve the kinematic redundancy in upper limb exoskeletons and, thus, generate human-like trajectories, improving the human-machine interaction.

Acknowledgements

I would like to thank the committee of the ETH Robotics Student Fellowship for giving me the opportunity of being selected to be part of this internship. I thank all the people from the Sensory-Motor Systems Lab, for giving me a warm welcome. Special thanks to Dr. Robert Reiner, Dr. Peter Wolf, and my mentors Yves Zimmerman and Michael Sommerhalder, who helped me to make the most of my time at the SMS Lab. Also, I want to thank my supervisors Dr. Joel Huegel and Dr. Mariana Ballesteros for being of inspiration and guide in my professional career. Last but not least, I thank God, my mom, dad and family, for supporting me at every moment.

References

- [1] Giuseppe Averta, Federica Barontini, Vincenzo Catrambone, Sami Haddadin, Giacomo Handjaras, Jeremia P O Held, Tingli Hu, Eike Jakubowitz, Christoph M Kanzler, Johannes Kühn, Olivier Lambery, Andrea Leo, Alina Obermeier, Emiliano Ricciardi, Anne Schwarz, Gaetano Valenza, Antonio Bicchi, and Matteo Bianchi. U-Limb: A multi-modal, multi-center database on arm motion control in healthy and post-stroke conditions. *GigaScience*, 10(6), 06 2021. giab043.
- [2] Andrea Maria Zanchettin, Luca Bascetta, and Paolo Rocco. Achieving humanlike motion: Resolving redundancy for anthropomorphic industrial manipulators. *IEEE Robotics Automation Magazine*, 20(4):131–138, 2013.
- [3] Nathanaël Jarrassé, Tommaso Proietti, Vincent Crocher, Johanna Robertson, Anis Sahbani, Guillaume Morel, and Agnès Roby-Brami. Robotic exoskeletons: A perspective for the rehabilitation of arm coordination in stroke patients. *Frontiers in Human Neuroscience*, 8, 2014.
- [4] Hyunchul Kim, Levi Makaio Miller, Aimen Al-Refai, Moshe Brand, and Jacob Rosen. Redundancy resolution of a human arm for controlling a seven dof wearable robotic system. In *2011 Annual International Conference of the IEEE Engineering in Medicine and Biology Society*, pages 3471–3474, 2011.
- [5] Mark L. Latash, John P. Scholz, and Gregor Schöner. Toward a new theory of motor synergies. *Motor Control*, 11(3):276 – 308, 2007.
- [6] Giuseppe Averta, Gaetano Valenza, Vincenzo Catrambone, Federica Barontini, Enzo Pasquale Scilingo, Antonio Bicchi, and Matteo Bianchi. On the time-invariance properties of upper limb synergies. *IEEE Transactions on Neural Systems and Rehabilitation Engineering*, 27(7):1397–1406, 2019.
- [7] N Hogan. An organizing principle for a class of voluntary movements. *Journal of Neuroscience*, 4(11):2745–2754, 1984.
- [8] Seungsu Kim, Changhwan Kim, and Jong Hyeon Park. Human-like arm motion generation for humanoid robots using motion capture database. In *2006 IEEE/RSJ International Conference on Intelligent Robots and Systems*, pages 3486–3491, 2006.
- [9] Tao Kang, Y. Shimansky, and Jiping He. Angle of elbow elevation depends on the reach target coordinates. In *Proceedings of the Second Joint 24th Annual Conference and the Annual Fall Meeting of the Biomedical Engineering Society] [Engineering in Medicine and Biology*, volume 3, pages 2571–2572 vol.3, 2002.

- [10] Hyunchul Kim, Jay Ryan Roldan, Zhi Li, and Jacob Rosen. Viscoelastic model for redundancy resolution of the human arm via the swivel angle: Applications for upper limb exoskeleton control. In *2012 Annual International Conference of the IEEE Engineering in Medicine and Biology Society*, pages 6471–6474, 2012.
- [11] Yves Zimmermann, Alessandro Forino, Robert Riener, and Marco Hutter. Anyexo: A versatile and dynamic upper-limb rehabilitation robot. *IEEE Robotics and Automation Letters*, 4(4):3649–3656, 2019.
- [12] Giuseppe Averta, Cosimo Della Santina, Gaetano Valenza, Antonio Bicchi, and Matteo Bianchi. Exploiting upper-limb functional principal components for human-like motion generation of anthropomorphic robots. *J. Neuroeng. Rehabil.*, 17(1), December 2020.
- [13] Axis-angle representation, Nov 2022.
- [14] "Bob McGinty.